IEEE Access
Multidisciplinary ⋮ Rapid Review ⋮ Open Access Journal

Received 24 July 2023, accepted 4 August 2023, date of publication 9 August 2023, date of current version 15 August 2023.

Digital Object Identifier 10.1109/ACCESS.2023.3303478

RESEARCH ARTICLE

A New FDTD Model for Lightning Return Stroke Channel Above Lossy Ground and Its Validation With Rocket-Triggered Lightning Data

GE ZHANG[1], MINGLI CHEN[1], SHAOYANG WANG[1], (Graduate Student Member, IEEE), YAN GAO[2], AND YA-PING DU[1]

[1]Department of Building Environment and Energy Engineering, The Hong Kong Polytechnic University, Hong Kong, SAR, China
[2]Guangdong-Hong Kong-Macao Greater Bay Area Weather Research Center for Monitoring Warning and Forecasting, Shenzhen 518038, China

Corresponding author: Mingli Chen (mingli.chen@polyu.edu.hk)

This work was supported in part The Hong Kong Polytechnic University through the Research Grants Council of Hong Kong under Grant GRF15215120 and in part by the National Natural Science Foundation of China under Grant 42105085.

ABSTRACT FDTD method has been widely used in calculations of electromagnetic fields produced by a lightning return stroke and its effects on other systems. However, the traditional Pi-type distributed resistance (R) – inductance (L) – capacitance (C) model representing a lightning return stroke is no longer suitable for FDTD method. In this study, we propose a new type *RLC* model that consists of a current source at the lightning channel base feeding a series of passive *RLC* loads above. The lightning return stroke channel is divided into small segments; each segment is presented by a height-dependent R in series with an L and in parallel with a C. With a current waveform measured for a return stroke in a rocket-triggered lightning discharge as the current source, impacts of different *RLC* settings on the channel current distribution properties were studied. Results show that the value of R has a significant impact on the attenuation pattern of both the current amplitude and propagation speed along the channel. Values of L and C have more impacts on the rising and falling edge of the current waveform and current propagation speed along the channel. The model was then applied to two sets of channel base currents and multi-station electric field measurements from two return strokes in rocket-triggered lightning experiments. By fitting the simulated electric field with the measured electrical field at each station, an optimal set of lightning channel *RLC* values for each of the two return strokes were determined, and hence the current propagation speed and amplitude as a function of the channel height were successfully estimated. The results show that both the current speed and amplitude decreased exponentially with the increase of the channel height, which are well consistent with existing optical observations and physical predictions in literature.

INDEX TERMS FDTD method, lightning return stroke, RLC model, rocket-triggered lightning, lightning electromagnetic pulse.

I. INTRODUCTION

Lightning discharge has been widely studied since the 20th century, of which the lightning return stroke is the most studied process. Based on large amount of optical and electromagnetic measurements, scientists have proposed various types of models for simulative studies of the lightning return stroke process [1]. Coming into 21st century, with the rapid development in computing technique, the Finite-Difference Time Domain (FDTD) method (a method to solve Maxwell equations with numerical techniques) has been widely used for the study of electrical effects caused by a lightning return stroke on various systems or objects [2].

To simulate the lightning effects more realistically, an adequate method representing a lightning return stroke in 3-dimension in FDTD method is important. A simple model

The associate editor coordinating the review of this manuscript and approving it for publication was Diego Bellan.

is to use a perfectly conducting short vertical wire (∼200 m long) with a lumped current source at its base to represent a lightning return stroke channel in FDTD method [3]. A self-defined current waveform is injected to the wire at its bottom. The current waveforms at different heights along the channel can then be simulated. Alternatively, the lightning return stroke channel could be represented with a vertical phased current-source array on a perfectly conducting plane. The current sources in the array have the same current waveforms but different phase delays. In both models, the current propagates along the lightning channel without any attenuation and the propagation speed is equal to the speed of light [3], which is far different from a true lightning return stroke channel. Nevertheless, such type of models has been widely used for investigations of lightning return stroke effects with FDTD, e.g. [4], [5], [6], [7], [8], and [9].

To better simulate the lightning current propagation velocity along the channel in FDTD, a model that a vertical perfectly conducting wire with and without additional distributed series of inductance was proposed [10]. Results of this type of models showed that the current propagation velocity along the channel could be altered by the inductance. However, attenuation trends of the current amplitude and propagation velocity along the channel were less pronounced. E.g.: [11] and [12].

There are two other types of models that can better represent a lightning return stroke in FDTD simulations. One is to use the dielectric material or medium to configure a vertical antenna to represent a return stroke channel above ground [13]. Another is to use a vertical wire coated by fictitious material to represent a return stroke channel above ground [14]. A recent research showed that these models could simulate reasonably the current propagation speed and the trend of change of the current amplitude along the lightning channel by choosing specific values of the permeability and permittivity of the dielectric material [15]. However, they still only yield a constant current propagation speed, and it is a time-consuming work to configure a specific lightning channel for a specific lightning case.

Nowadays, many researchers are using a vertical current-source array to represent a lightning return stroke in their FDTD simulations. The current sources at different channel heights in the array are calculated based on the Modified Transmission-Line Model (MTLM) with a constant current propagation speed and a linear decay of current amplitude along the lightning channel [16], [17], [18], [19]. The current waveform used in these model were either an artificially generated Gauss waveform or from an analytical representation of measured lightning current [20]. To certain extents, this kind of models can represent a lightning return stroke channel in 3D in FDTD simulations properly but cannot realistically simulate the lightning current propagation and attenuation properties along the channel.

Observations show that both the amplitude and propagation speed of the lightning current attenuate nonlinearly as it propagates along its channel, which can be simulated with none of above models. On the other side, the current speed along with the current peak largely determines the initial peak of radiation field produced by a return stroke. Therefore, it is quite necessary to have a model that can well represent a lightning return stroke channel for accurate calculations of lightning-produced electromagnetic fields with FDTD method.

In this study, we propose and practice a longitudinal-dependent resistance (R) -inductance (L) -capacitance (C) model to present a lightning return stroke above a lossy ground in 3D in FDTD simulations. The lightning channel is simulated by a current source at the channel base with a series of height-dependent *RLC* load above. With different settings of *RLC* parameters for a given base current source, different current propagation and attenuation properties along the channel can be simulated. As such, a lightning return stroke channel with different current properties can be simulated in 3D with a high flexibility and accuracy. With the model, different lightning current propagation and attenuation properties and their impacts on the lighting-produced electric fields at different distances were investigated. The model was then validated with and applied to the channel base currents and associated multi-station electric field changes measured for lightning return strokes in rocket-triggered lightning flashes during the Guangdong Comprehensive Observing Experiment on Lightning Discharge (GCOELD) [21]. For each of the cases studied, by tuning the *RLC* settings and fitting the simulated electric fields with the measured electric fields for the measured channel-based currents, the current amplitude and propagation speed as a function of the channel height were successfully retrieved, which is a good indicator of the high accuracy and practicability of the model we proposed.

II. METHODOLOGY

A. REPRESENTATION OF LIGHTNING RETURN STROKE CHANNEL IN FDTD CODE

An illustration of representation of the lightning return stroke channel in FDTD simulation is shown in Figure 1. The lightning channel is supposed to be H = 3000 m high above ground in this study, which is divided into 10 m × 300 segments, corresponding to a FDTD grid size of 10 m × 10 m × 10 m. Theoretically, the space resolution can be set to any a smaller value than this. We take the 10 m value because it is enough for the frequency bands of the current and electric field measurements used in this study, meanwhile can significantly save the computing cost. The 1st segment is grounded via a current source, and the 2nd and above segments are a series of passive loads numbered from No.1 to No.299. Each segment is equivalent to a passive load that consists of a resistance (R_i) in series with an inductance (L_i) and then in parallel with a capacitance (C_i), where $i = 1$ to 299 is the segment index. A real lightning return stroke current waveform obtained from GCOELD is used as the current source at the channel base, and the simulated electric fields on ground are compared with the measured ones to validate the model.

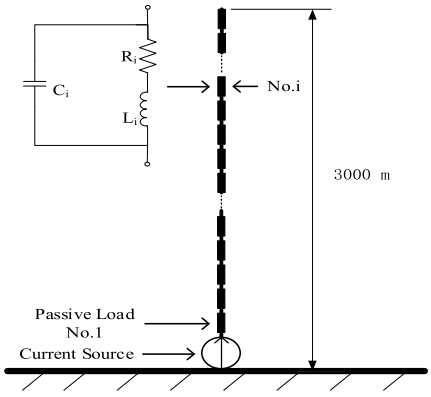

FIGURE 1. An illustration of the representation of a lightning return stroke channel in FDTD code.

We firstly presented the preliminary idea of this model at an international conference held in 2018, but with no details and accurate interpretation of the model [22]. As shown in Figure 1, the lightning channel is excited by a current source at the channel base. As the current propagates upward, the charge deposits into capacitance due to the voltage drop cross inductance and resistance at each segment of the passive loads. The charge distribution and current propagation and attenuation properties along the lightning channel can then be simulated with adequate *RLC* values. While the capacitance (C_i) in each segment is supposed to be the same (C_0), the resistance (R_i) and inductance (L_i) in each segment are supposed to increase with the increase of the channel height, which is given by equations (1) to (3). By tuning the values of the resistance, inductance and capacitance, lightning return strokes with different channel current properties can be represented.

$$R_i = \Delta H \cdot R_0 \cdot (1 + \Delta H \cdot \Delta R_0\%)^{i-1} \quad (1)$$

$$L_i = \Delta H \cdot L_0 \cdot (1 + \Delta H \cdot \Delta L_0\%)^{i-1} \quad (2)$$

$$C_i = C_0 \quad (3)$$

where, R_0 (in Ω/m) and L_0 (in μH/m) are the initial values for the resistance and inductance, respectively, for the first passive load above the current source at the channel base. ΔR_0 and ΔL_0 are the increasing rates (in percentage per meter) for the resistance and inductance along the channel, respectively. ΔH (in meter) is the length of each segment/passive load, which is 10 m in this study. C_0 (in μF) is the value of the capacitance, which is the same for all segments. Determinations of the values of these five parameters are explained in detail in next session.

B. DETERMINATION OF LIGHTNING RETURN STROKE CHANNEL PARAMETERS

In this height-dependent *RLC* model, determinations of the five parameters are essential to properly represent a specific lightning return stroke channel in 3D. For the initial values of the resistance R_0, inductance L_0 and capacitance C_0, the empirical and theoretical results in many previous investigations on lightning return stroke modeling can be referenced, e.g.: [10], [13], [23], and [24]. According to those studies, R_0 should be theoretically in the order of 3 Ω/m, and L_0 should be in the order of 1 μH/m. For the capacitance, it is generally assumed to be about 7 pF/m in most of the Pi-type *RLC* transmission line model for a lightning return stroke, where the capacitance for each channel segment is grounded and connected in parallel to each other [23], [24]. In contrast, the capacitance for each segment in the present model is not grounded and connected in series to each other. As such, the theoretical value of C_0 in the present model should be in the order of (300 segments) times (7 pF) = 0.002 μF.

About the increasing rate of resistance and inductance (ΔR_0 and ΔL_0) and the capacitance (C_0), as we know that both the leader and return stroke channels are consisted of a conductive core surrounded by a corona sheath. While the resistance and inductance largely depends on the conductive core, the channel capacitance largely depends on the dielectric property of the corona sheath. Both observation and theoretical analysis show that the lightning return stroke current decreases significantly in its amplitude and propagation speed when it propagates upward along the channel. From the point of view of physical process, the wave front of a lightning return stroke current usually propagates upward along the residual channel of a preceding downward leader. The residual channel of a downward leader usually has a thinner and cooler conductive core at upper parts of the channel and a thicker and hotter conductive core at lower parts of the channel. All these imply that the lightning return stroke channel has an equivalent resistance and inductance that may increase with the increase of the channel height. The values of ΔR_0 and ΔL_0 should be at such a level so that the amplitude of the current pulse will be attenuated to a very low level when it reaches the channel top to avoid obvious reflections of current waves there, which are set to be about 0.05%/m in this study. Since the dielectric property of the corona sheath usually do not fluctuate significantly along the channel during a given lightning event, the channel capacitance may be set as a constant along the channel reasonably.

The actual values of the channel *RLC* in the model may vary case by case, depending on how the lightning current is distributed on the lightning channel. In another words, we may simulate the current distribution property along a specific lightning channel by tuning *RLC* values in certain ranges, so that the modelled currents and electromagnetic fields can well match with observations. In general, R_0 plus ΔR_0 has more influences the current attenuation pattern along the lightning channel, while L_0 and C_0 have more influences on the current waveform and propagation speed. Detailed analyses on how the *RLC* values affect the current propagation properties and electric field waveforms at different distances on ground are given in section III-A.

C. VERIFICATION AND APPLICATION OF THE LIGHTNING RETURN STROKE MODEL

For verification and application of the model, two sets of channel based current and on-ground vertical electrical field

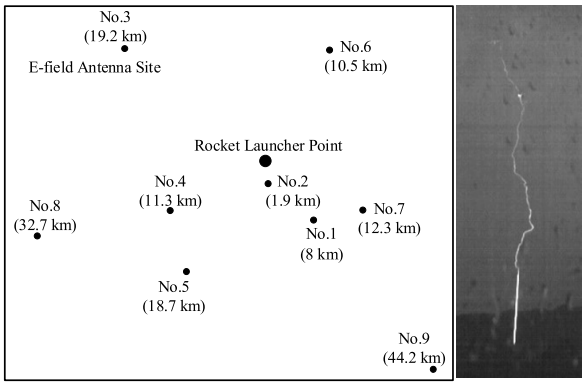

(a) Sketch of E-field antenna sites around the rocket launcher (right) and a typical image of a rocket-triggered lightning return stroke (left).

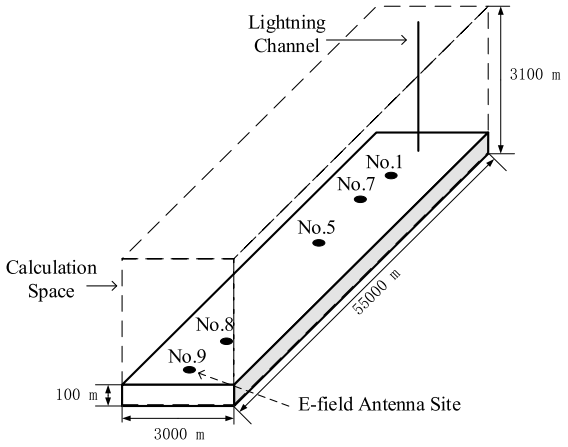

(b) Space setting for testing of the return stroke model in FDTD

FIGURE 2. Lightning measurements and FDTD modelling settings.

measurements for lightning return strokes in rocket-triggered lightning experiments during GCOELD were used [21]. The measurements included lightning channel base currents measured at the rocket launcher position and on-ground multi-station electric field changes at different distances ranged from 1 km to 45 km around the rocket launcher, as shown in Figure 2a. According to the measurement arrangements and for reducing the computing cost, the FDTD calculation space was set to 55 km (long) × 3 km (wide) × 3.1 km (high), as shown in Figure 2b.

The lightning return stroke channel is supposed to vertically stand on a flat ground with a soil layer thickness of 100 m. The electric field sensors were located at different distances from the lightning channel based on the actual situation during the rocket-triggered lightning experiments. For a specific current measured at the channel base of a lightning return stroke, the current channel distributions and hence the lightning-produced electric fields at different distances on ground were calculated with different channel *RLC* settings. The *RLC* setting whose outputs of the electric fields best match with the electrical field measurements was then considered as the best one to represent that lightning channel, and the corresponding calculated current channel distributions were considered to represent the current propagation and attenuation properties along the channel of that lightning return stroke. Detailed results and analyses are given in section III-B.

III. MODELING RESULTS AND ANALYSIS

A. EFFECTS OF CHANNEL RLC SETTINGS ON CHANNEL CURRENTS AND GROUND E-FIELDS

The model consists of five parameters: R_0, L_0, C_0, ΔR_0 and ΔL_0. Reasonable value ranges of the five parameters were discussed in section II-B. In this section, several sets of specific parameter values around the reasonable value ranges are chosen to make up different lightning return stroke channels. With the same base current waveform, the channel current propagation and attenuation properties under different channel parameter settings are simulated with the model. The lightning-produced electric fields (E-fields) at a medium-close distance of 5 to 15 km, which usually consist of obvious electrostatic, inductive, and radiative field components, are well suitable to reflect the current propagation and attenuation properties along a lightning channel. For this sake, the E-fields at a distance of 8 km (corresponding to site No.1) from the lightning channel base under different channel parameter settings are calculated. The base current waveform used in this section was measured for a return stroke occurred at 18h29min (Beijing time) on 11 June 2015 from GCOELD, which has a peak value of 9.2 kA. The ground conductivity used in this section is the same 0.005 S/m, a typical value for dry soil at GCOELD. We also tested the value of 0.05 S/m, but the result showed little difference from the present one. This is because that the E-field in a LF/VLF band is not so sensitive to the soil conductivity in the range from 0.05 S/m to 0.005 S/m. By comparing the results under different model parameter settings, effects of the five parameters on the current properties and the E-field waveforms are investigated.

1) THE EFFECT OF CHANNEL RESISTANCE R_0 AND ΔR_0

Shown in Figure 3 are the modelling results of lightning channel currents and ground E-fields for 3 different R_0 values (4, 5 and 6 Ω/m) with the same L_0 (0.5 μH/m), C_0(0.002 μF), ΔR_0(0.05%/m), ΔL_0(0.05%/m) and ground conductivity (0.005 S/m) for the same channel base current measured for a return stroke in GCOELD on 11 June 2015. The current propagation speed is estimated based on the timing of maximum change rate of the current rising front at each segment along the lightning channel. As shown in the figure, both the current amplitude and speed decrease exponentially as it propagates along the channel upward, which are well consistent with expectations. A larger R_0 leads to a larger decreasing rate of both the current amplitude and speed along the channel, resulting in a smaller amplitude of the E-field on ground. Increasing the R_0 value has no more impact on the rising edge of the E-field waveform but makes the falling edge of the waveform sharper. This means that a larger

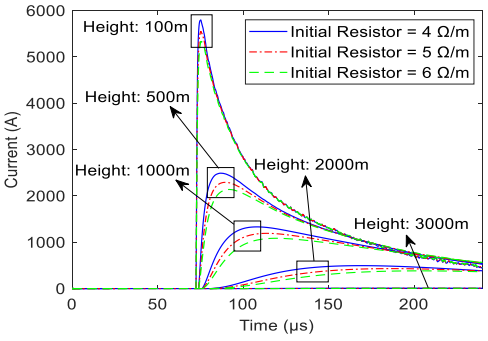

(a) Current versus channel heights

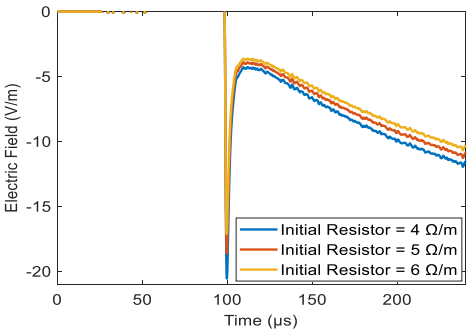

(b) Electric field at 8 km apart

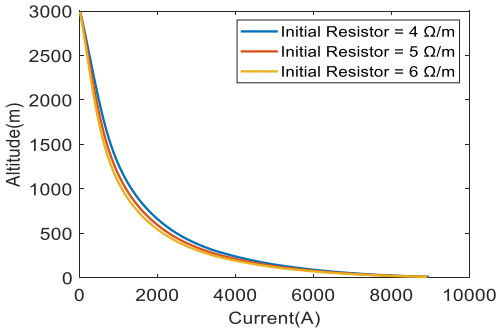

(c) Current peak versus channel heights

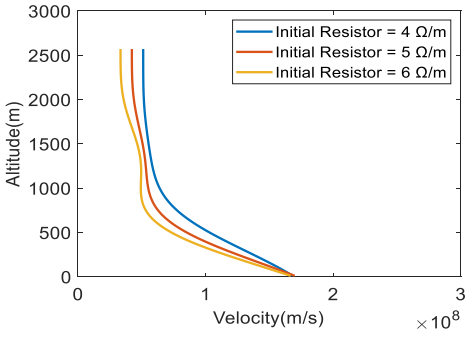

(d) Current speed versus channel heights

FIGURE 3. Modelling results of lightning channel currents and ground E-fields for 3 different R_0 values (4, 5 and 6 Ω/m) with the same L_0 (0.5 μH/m), C_0 (0.002 μF), ΔR_0% (0.05%/m), ΔL_0% (0.05%/m) and ground conductivity (0.005 S/m) for the same channel base current measured for a return stroke in GCOELD on 11 June 2015.

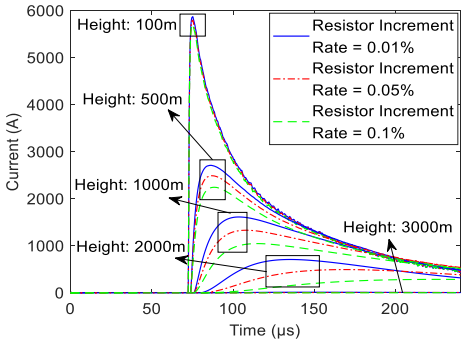

(a) Current versus channel heights

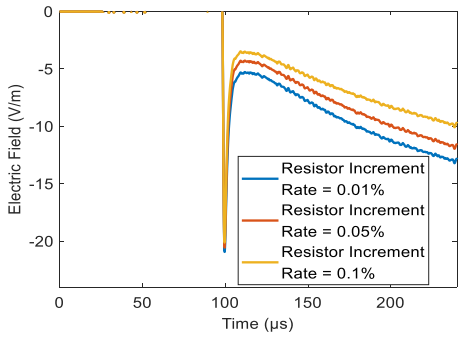

(b) Electric field at 8 km apart

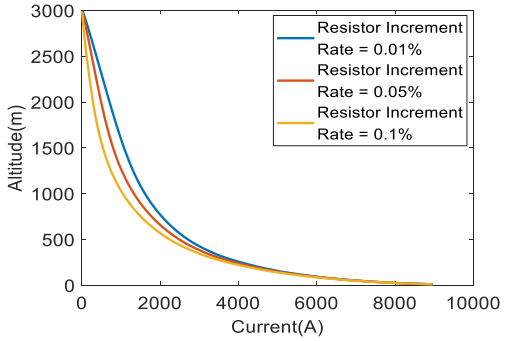

(c) Current peak versus channel heights

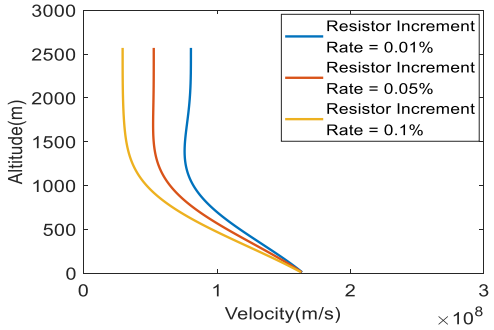

(d) Current speed versus channel heights

FIGURE 4. Modelling results of currents and E-fields for 3 different ΔR_0 values (0.01%/m, 0.05%/m and 0.1%/m) with the same R_0 (4 Ω/m), L_0 (0.5 μH/m), C_0 (0.002 μF), ΔL_0 (0.05%/m) and ground conductivity (0.005 S/m) for the same channel base current as in Figure 3.

channel resistance causes a faster decreasing of the amplitude and speed of the current along the channel, resulting in a smaller amplitude and a faster falling edge of the E-field waveform.

Shown in Figure 4 are the modelling results of channel currents and ground E-fields for 3 different ΔR_0 values (0.01%/m, 0.05%/m and 0.1%/m) with the same R_0 (4 Ω/m), L_0 (0.5 μH/m), C_0 (0.002 μF), ΔL_0 (0.05%/m) and ground conductivity (0.005 S/m) for the same channel base current as in Figure 3. It shows that a larger ΔR_0 leads to a larger decreasing rate of current amplitude and propagation speed at upper parts of the lightning channel. As a result, the ΔR_0 value has a little influence on the peak of the E-field waveform (which is dominated by the radiative field), but a big influence on the tail of the E-field waveform (which is dominated by static field). A larger ΔR_0 leads to a smaller amplitude of the tail of the E-field waveform.

2) THE EFFECT OF CHANNEL INDUCTANCE L_0 AND ΔL_0

Shown in Figure 5 are the modelling results of currents and E-fields for 3 different L_0 values (0.5, 1 and 1.5 μH/m) with the same R_0 (4 Ω/m), C_0 (0.002 μF), ΔR_0 (0.05%/m), ΔL_0 (0.05%/m) and ground conductivity (0.005 S/m) for the same channel base current as in Figure3. It shows that the L_0 value has a little influence on the channel current distribution and hence the ground E-field waveform. In general, a larger L_0 value leads to a relatively higher peak and a slower rising and falling edge of the current waveform, but the difference is small. An obvious effect is that a larger L_0 value leads to a lower current speed at lower parts of the channel. As a result, a larger L_0 value results in a relatively smaller peak and a slower rising and falling edge of the E-field waveform, with no more influence on tail parts of the E-field.

Shown in Figure 6 are the modelling results of currents and E-fields for 3 different ΔL_0 values (0.01%, 0.05% and 0.1%/m) with the same R_0 (4 Ω/m),L_0 (0.5 μH/m), C_0 (0.002 μF), ΔR_0 (0.05%/m) and ground conductivity (0.005 S/m) for the same channel base current as in Figure3. It shows that changing the ΔL_0 value has a negligible influence on the channel current distribution and hence the E-field waveform. Although different ΔL_0 values may lead to big differences in inductance at upper parts of the channel, the calculated E-field waveforms rarely show their differences at least at this distance (8 km from the channel base). The E-fields at further distances are given in part B of this section.

3) THE EFFECT OF CHANNEL CAPACITANCE C_0

Shown in Figure 7 are the modelling results of currents and E-fields for 3 different C_0 values (0.001, 0.002 and 0.003 μF) with the same R_0 (4 Ω/m), L_0 (0.5 μH/m),ΔR_0 (0.05%/m), ΔL_0 (0.05%/m) and ground conductivity (0.005 S/m) for the same channel base current as in Figure 3. It shows that changing the C_0 value has a little influence on the channel current distribution and hence the E-field. In general, a larger C_0 leads to a relatively smaller peak and a faster rising and falling edge of the current waveform, but the difference is not obvious. An important effect is that a larger C_0 leads to a higher current speed along the whole channel. As a result, a larger C_0 results in a relatively smaller peak and a faster rising and falling edge of the E-field waveform, with no more influence on the waveform tail.

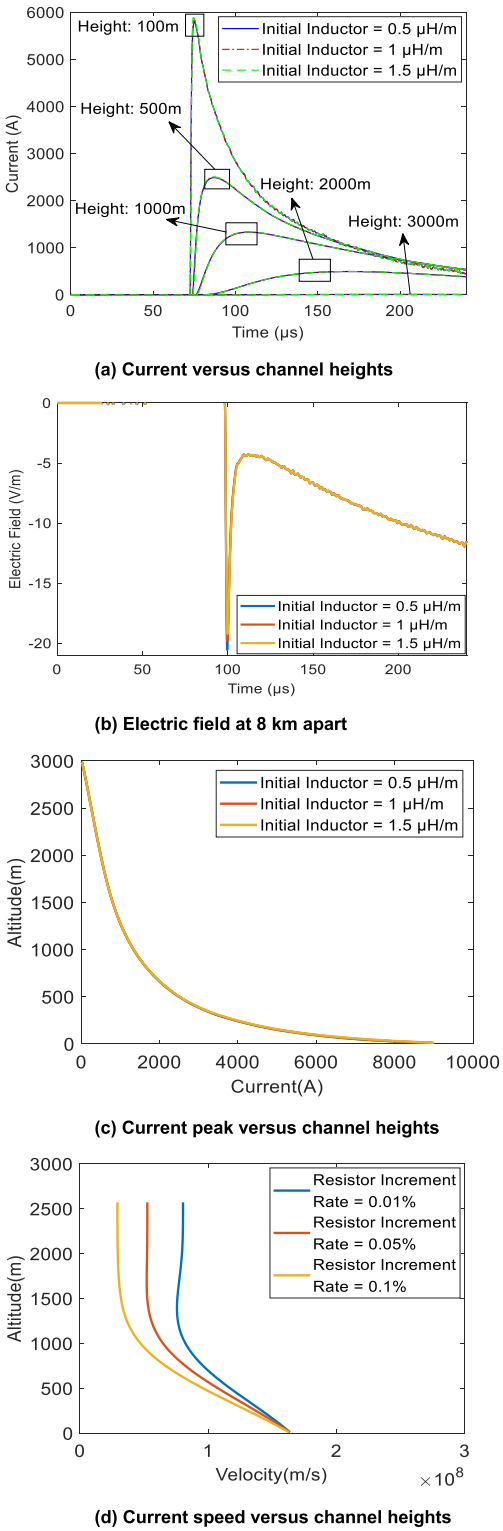

(a) Current versus channel heights

(b) Electric field at 8 km apart

(c) Current peak versus channel heights

(d) Current speed versus channel heights

FIGURE 5. Modelling results of currents and E-fields for 3 different L_0 values (0.5, 1 and 1.5 μH/m) with the same R_0 (4 Ω/m), C_0 (0.002 μF), ΔR_0 (0.05%/m), ΔL_0 (0.05%/m) and ground conductivity (0.005 S/m) for the same channel base current as in Figure 3.

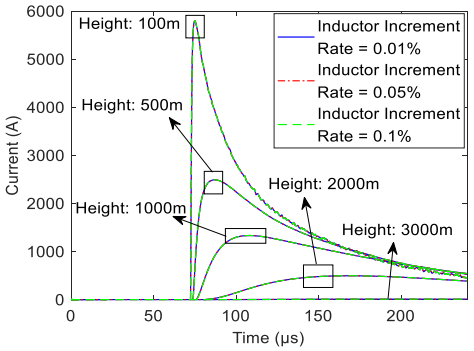

(a) Current versus channel heights

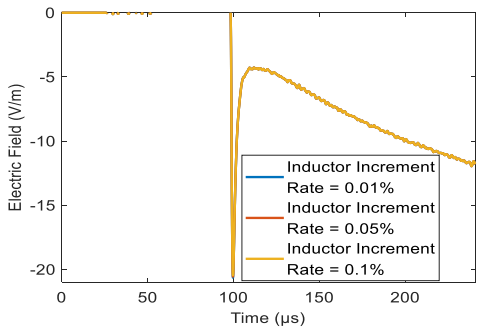

(b) Electric field at 8 km apart

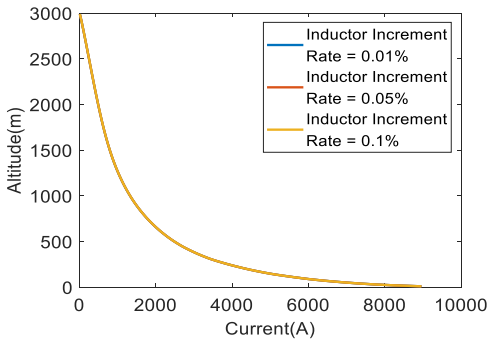

(c) Current peak versus channel heights

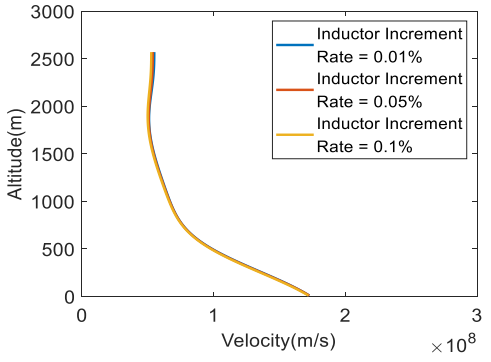

(d) Current speed versus channel heights

FIGURE 6. Modelling results of currents and E-fields for 3 different ΔL_0 values (0.01%, 0.05% and 0.1%/m) with the same of R_0 (4 Ω/m), L_0 (0.5 μH/m), C_0 (0.002 μF), ΔR_0 (0.05%/m) and ground conductivity (0.005 S/m) for the same channel base current as in Figure 3.

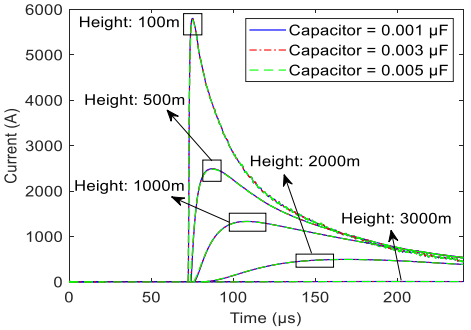

(a) Current versus channel heights

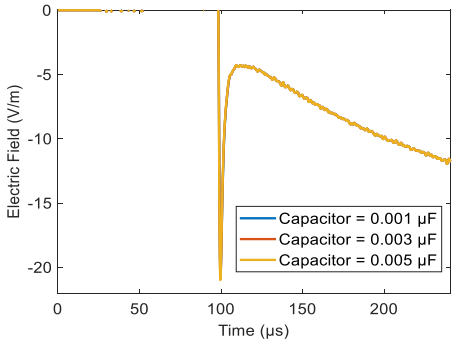

(b) Electric field at 8 km apart

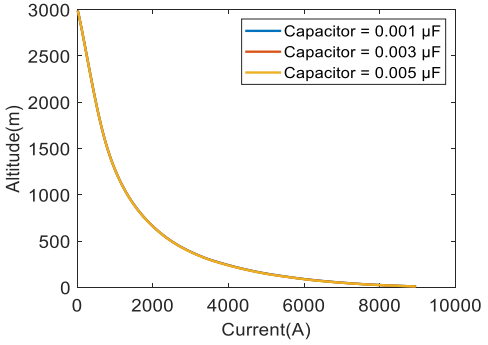

(c) Current peak versus channel heights

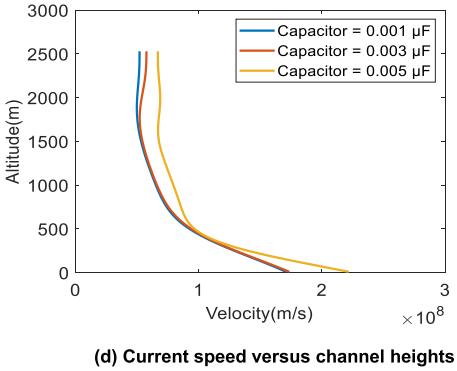

(d) Current speed versus channel heights

FIGURE 7. Modelling results of currents and E-fields for 3 different C_0 values (0.001, 0.003 and 0.005 μF) with the same R_0 (4 Ω/m), L_0 (0.5 μH/m),ΔR_0 (0.05%/m), ΔL_0 (0.05%/m) and ground conductivity (0.005 S/m) for the same channel base current as in Figure 3.

In summary, the channel resistance plays a dominant role affecting the current attenuation rate (both the amplitude and speed) along the channel. A larger R_0 leads to a bigger attenuation rate of the current along the channel, while a larger

TABLE 1. The site information of buildings where the 5 E-field are installed on and the local site enhancement coefficient of the E-field estimated.

E-field Antenna Site No.	Building Size (Wide*Long*High)	Enhancement Coefficient (E-field, peak)	Enhancement Coefficient (E-field, tail)	Distance from Rocket Launcher
No.1	30m*45m*10m	1.34	1.34	8.0 km
No.5	30m*10m*10m	1.41	1.40	18.7 km
No.7	25m*20m*20m	1.82	1.81	12.3 km
No.8	10m*35m*10m	1.44	1.47	32.7 km
No.9	30m*30m*20m	1.62	1.62	44.2 km

ΔR_0 leads to a much bigger current attenuation rate at upper parts of the channel. The channel inductance and capacitance have an ignorable influence on the current amplitude, but an observable influence on the current waveforms and a big influence on the current propagation speeds. A larger L_0 leads to a wider current waveform along the channel and a lower current speed at lower parts of the channel, while a larger C_0 leads to a narrower current waveform and a faster current speed along the whole channel.

B. APPLICATION AND VALIDATION OF THE MODEL

The model are applied to two sets of channel base current and multi-station E-field measurements from two return strokes in GCOELD for verification of the model. The base currents were measured with a coaxial shunt of 1 mΩ (bandwidth 200 MHz) mounted at the rocket launcher site and recorded on a digital oscilloscope at a sampling rate of 10 MS/s [21]. The E-fields were measured with a so-called Low-frequency E-field Detection Array (LFEDA), which consisted of 9 stations, each station was equipped with a fast E-field antenna having a bandwidth of 160 Hz to 600 kHz and a time constant of 1 ms [25]. The E-field measurements from 5 out of the 9 stations are available for this study. Site information of the 5 E-field antennas is summarized in Table 1.

1) CASE 1

The channel base current of Case 1 was measured from the first return stroke in a rocket-triggered lightning flash occurred at 18h29min (Beijing time) on 11 June 2015 during GCOELD, which has a current peak of 9234 A. By fitting the calculated E-fields with the measured E-field at Site No.1 for this case, a reasonable set of lightning channel parameters is found as: $R_0 = 4$ Ω/m, $L_0 = 0.5$ μH/m, $C_0 = 0.002$ μF, $\Delta R_0\% = 0.08\%$/m and $\Delta L_0\% = 0.05\%$/m. It should be mentioned that the sampling rate of both the current and E-field measurements was 10 MHz. To ensure the accuracy of the simulation results, all measurements and calculated currents and E-fields presented here are processed with a 2 MHz low- pass filter.

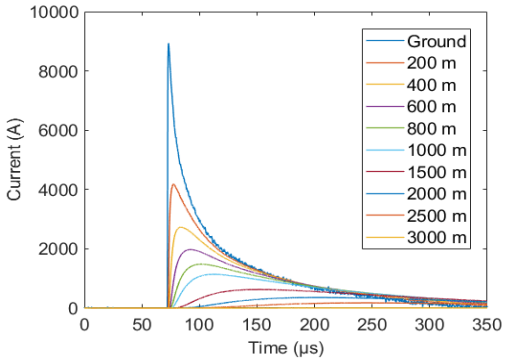

(a) Currents versus heights for Case 1

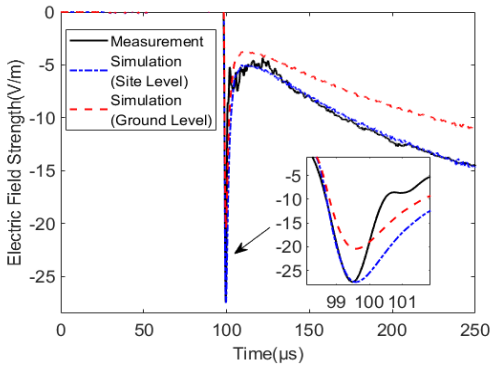

(b) E-field for Site No.1 at 8 km for Case 1

FIGURE 8. (a) The measured channel base current (- Ground) and the simulated current versus channel height, and (b) a comparison of the measured E-field on building top (- Measurement) with the simulated E-field on building top (- simulation site level) and that on ground level (- simulation ground level) for Site No.1, for Case 1.

Shown in Figure 8(a) is the measured base current and simulated current distributions along the lightning channel for Case 1, which shows that the channel current attenuates exponentially as it propagates along the channel upwards. Shown in Figure 8(b) is a comparison of the measured E-field on the building top with the simulated E-field on the building top and that on the ground level at Site No.1 for Case 1. It is noted while the simulated E-field on the building top is well fitted with the measured E-field there, its amplitude is much bigger that of the simulated E-field on ground level, which is due to the local E-field enhancement on the building. To address this effect, we define two E-field enhancement coefficients: the ratio of peak of the E-field waveform on the building top to that on the ground level, and the ratio of tail amplitude of the E-field waveform on the building top to that on the ground level. The enhancement coefficient for the E-field peak and tail for Site No.1 is the same 1.34.

Similar to Site No.1, shown in Figures 9 are the comparisons of the measured and simulated E-fields for Site No. 5, No.7, No.8 and No.9, respectively. The two enhancement coefficients for the E-field peak and the tail for these sites are estimated and listed in Table 1.

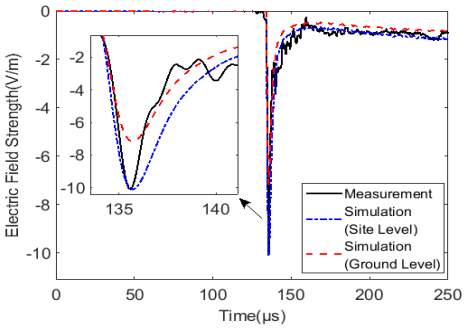

(a) E-field for Site No.5 at 18.7 km

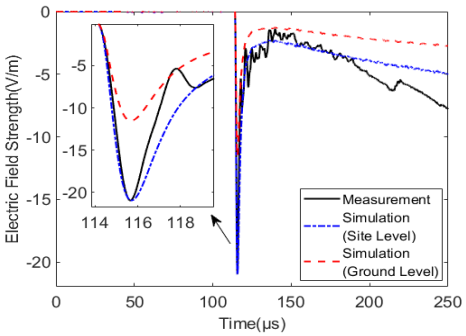

(b) E-field for Site No.7 at 12.3 km

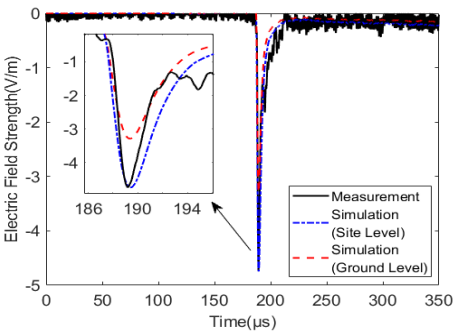

(c) E-field for Site No.8 at 32.7 km

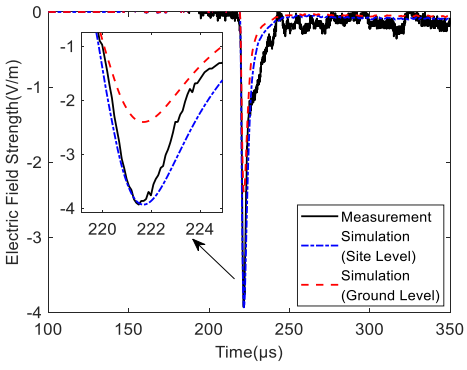

(d) E-field for Site No.9 at 44.2 km

FIGURE 9. A comparison of the measured E-field on building top with the simulated E-field on building top and that on ground level, for (a) Site No.5, (b) Site No. 7, (c) Site No. 8 and (d) Site No.9, for Case 1.

2) CASE 2

The channel base current of Case 2 was measured from the second return stroke in a rocket-triggered lightning flash

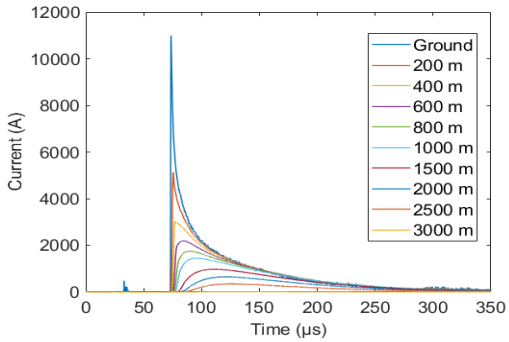

(a) Currents versus heights for Case 2

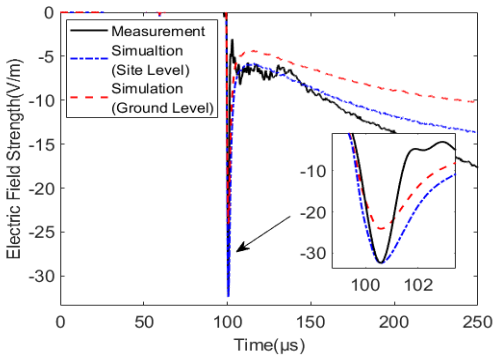

(b) E-field for Site No.1 at 8 km for Case 2

FIGURE 10. (a) The measured channel base current (- Ground) and the simulated current versus channel height, and (b) a comparison of the measured E-field on building top (- Measurement) with the simulated E-field on building top (- Simulation site level) and that on ground level (- Simulation ground level) for Site No.1, for Case 2.

occurred at 18h22min (Beijing time) on 11 June 2015 during GCOELD, which has a current peak of 10678 A. By fitting the calculated E-fields with the measured E-field at Site No.1, the reasonable lightning channel parameters found for this case are: $R_0 = 3$ Ω/m, $L_0 = 1.4$ μH/m, $C_0 = 0.002$ μF, $\Delta R_0\% = 0.01\%$/m and $\Delta L_0\% = 0.05\%$/m. It is noted the values of resistance and inductance for this case are different from those for Case 1, indicating the current attenuation and propagation property for this case is different from that for Case 1. Similar to Case 1, all measurements and calculated currents and E-fields presented here are processed with a 2 MHz low- pass filter.

Shown in Figure 10(a) are the measured base current and the simulated current distributions along the lightning channel for Case 2, from which the current attenuation rate and propagation speed could be estimated. Comparisons of the measured and simulated E-field for Site No.1, No.5, No.7, No.8 and No.9 for Case 2 are shown in Figure 10 (b) and Figures 11(a), (b), (c) & (b), respectively. The two E-field enhancement coefficients for these sites for Case 2 are estimated and listed in Table 1.

3) ATTENUATION PATTERNS OF CHANNEL CURRENT PEAK AND PROPAGATION SPEED

According to the simulated current waveforms at different heights along the channel shown in Figure 8(a) for Case 1 and

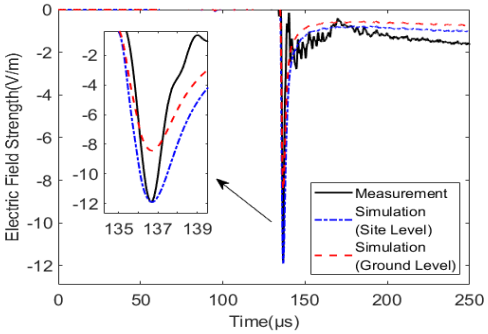

(a) E-field for Site No.5 at 18.7 km for Case 2

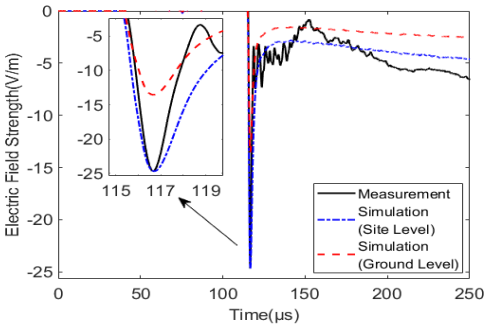

(b) E-field for Site No.7 at 12.3 km for Case 2

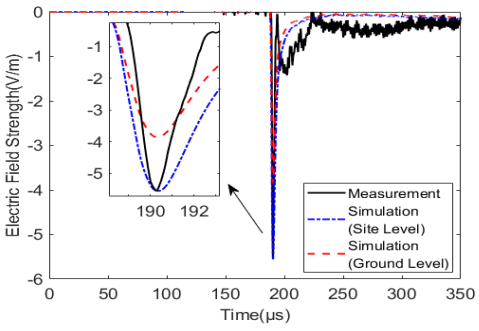

(c) E-field for Site No.8 at 32.7 km for Case 2

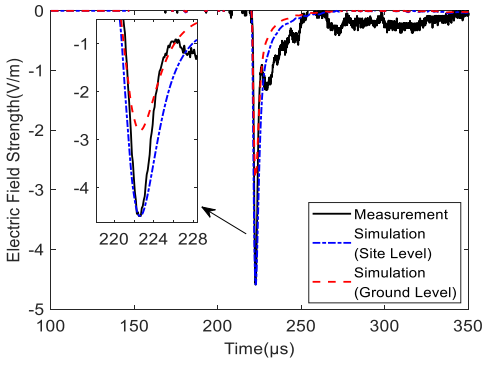

(d) E-field for Site No.9 at 44.2 km for Case 2

FIGURE 11. A comparison of the measured E-field on building top with the simulated E-field on building top and that on ground level, for (a) Site No. 5, (b) Site No. 7, (c) Site No. 8 and (d) Site No.9, for Case 2.

Figure 10(a) for Case 2, variations of the current peak and propagation speed versus the channel height are estimated, as shown in Figures 12(a)&(b), respectively.

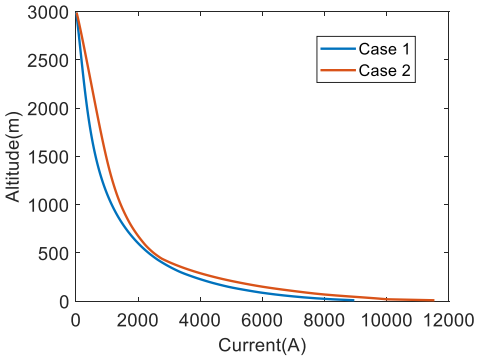

(a) Current peak versus heights

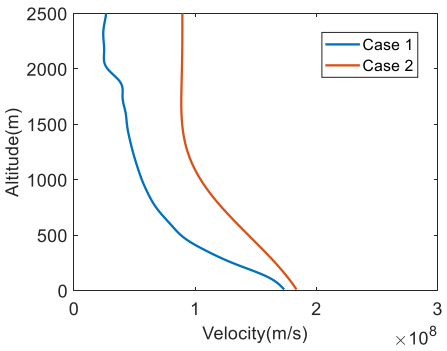

(b) Current speed versus heights

FIGURE 12. Attenuation patterns of (a) the current peak versus height and (b) current propagation speed versus height, calculated with the model for the two return strokes of Case 1 and Case 2.

As shown in the figure, the current peak attenuates exponentially with the increase of the channel height for both cases, but the attenuation rate is different case by case. The current propagation speed also shows an exponentially decreasing trend with the increase of the channel height for both cases, but the speed and its decreasing rate are quite different between the two cases. The current speed for Case 1 is about 1.74×10^8 m/s at ground level and then quickly decreases to 0.86×10^8 m/s at 500 m high and 0.26×10^8 m/s at 2500 m high. Whilst the current speed for Case 2 is about 1.84×10^8 m/s at ground level and then decreases to 1.42×10^8 m/s at 500 high and 0.89×10^8 m/s at 2500 m high. When the current propagates higher than 2500 m, the current rising front is too small and flat, therefore, there is no current speed estimated after that height. Typical values of return-stroke speed observed optically are in the range of $1.0 \sim 2.0 \times 10^8$ m/s [26], [27]. Our results are well consistent with the optical observations of the lightning return stroke speed as well as the physical modeling predictions in literature [28].

IV. CONCLUSION

A new *RLC* model for lightning return stroke channel representation in FDTD code was proposed. In the model, a lightning return stroke channel is represented by a current source at the channel base in series with a height-dependent

RLC load above the base. With a given base current and a reasonable set of the channel *RLC*values, the model result shows that both the current amplitude and propagation speed have an exponentially decreasing trend along the channel upward, which is well consistent with optical observations and physical predictions for lightning return strokes in literature.

With the current measured for a lightning return stroke in a rocket-triggered lightning discharge during GCOELD, impacts of various channel *RLC* settings on the current distributions along the channel were investigated. Results show that the channel resistance plays a dominant role affecting the attenuation pattern of both the current amplitude and propagation speed along the channel. A larger channel resistance leads to a larger current amplitude and speed attenuation rate along the channel. The channel inductance and capacitance have a little influence on the current waveform but a big influence on the current propagation speed. A larger inductance leads to a wider current waveform along the channel and a lower current speed at lower parts of the channel, while a larger capacitance leads to narrower current waveform and a faster current speed along the whole channel.

The model was then applied to two sets of channel base current and multi-station E-field measurements for two return strokes in artificially triggered lightning experiments. By fitting the measured and simulated E-fields, the optimal channel *RLC* setting for each of the two return strokes were determined, and hence the current distribution pattern along the channel were calculated. Results show that for both cases, the current peak attenuates exponentially along the channel upward, but the attenuation rate is different case by case. The current propagation speed also shows an exponentially decreasing trend along the channel upward for both cases, but the speed value and changing rate along the channel are quite different between the two cases. These results are well consistent with optical observations of the lightning return stroke propagation in literature.

There are at least two limitations of this model. 1) The resistance and inductance along the lightning are supposed to increase with the increase of the channel height linearly and the capacitance is supposed to be a constant along the channel, which may not reflect completely the real situation of lightning return stroke channel. 2) The frequency band we addressed in this study is limited to 2 MHz and the ground conductivity is set to a constant of 0.005 S/m, which is not good for examining the E-field response to various soil conductivities. Further works are needed to address these limitations.

ACKNOWLEDGMENT

The authors would like to thank colleagues of the Guangdong Rocket-Triggered Lightning Experiment Group for their supports in lightning data.

REFERENCES

[1] V. A. Rakov and M. A. Uman, "Review and evaluation of lightning return stroke models including some aspects of their application," *IEEE Trans. Electromagn. Compat.*, vol. 40, no. 4, pp. 403–426, Nov. 1998.

[2] Y. Baba and V. A. Rakov, "Applications of the FDTD method to lightning electromagnetic pulse and surge simulations," in *Proc. Int. Conf. Lightning Protection (ICLP)*, Oct. 2014, pp. 325–339.

[3] Y. Baba and V. A. Rakov, "On the transmission line model for lightning return stroke representation," *Geophys. Res. Lett.*, vol. 30, no. 24, pp. 1–4, Dec. 2003.

[4] D. Li, Q. Zhang, Z. Wang, and T. Liu, "Computation of lightning horizontal field over the two-dimensional rough ground by using the three-dimensional FDTD," *IEEE Trans. Electromagn. Compat.*, vol. 56, no. 1, pp. 143–148, Feb. 2014.

[5] D. Li, Q. Zhang, T. Liu, and Z. Wang, "Validation of the Cooray-Rubinstein (C-R) formula for a rough ground surface by using three-dimensional (3-D) FDTD," *J. Geophys. Res., Atmos.*, vol. 118, no. 22, pp. 749–754, Nov. 2013.

[6] A. Tatematsu, F. Rachidi, and M. Rubinstein, "Analysis of electromagnetic fields inside a reinforced concrete building with layered reinforcing bar due to direct and indirect lightning strikes using the FDTD method," *IEEE Trans. Electromagn. Compat.*, vol. 57, no. 3, pp. 405–417, Jun. 2015.

[7] T. H. Thang, Y. Baba, N. Nagaoka, A. Ametani, N. Itamoto, and V. A. Rakov, "FDTD simulation of insulator voltages at a lightning-struck tower considering ground-wire corona," *IEEE Trans. Power Del.*, vol. 28, no. 3, pp. 1635–1642, Jul. 2013.

[8] D. Li, M. Azadifar, F. Rachidi, M. Rubinstein, G. Diendorfer, K. Sheshyekani, Q. Zhang, and Z. Wang, "Analysis of lightning electromagnetic field propagation in mountainous terrain and its effects on ToA-based lightning location systems," *J. Geophys. Res., Atmos.*, vol. 121, no. 2, pp. 895–911, Jan. 2016.

[9] T. H. Thang, Y. Baba, N. Nagaoka, A. Ametani, N. Itamoto, and V. A. Rakov, "FDTD simulations of corona effect on lightning-induced voltages," *IEEE Trans. Electromagn. Compat.*, vol. 56, no. 1, pp. 168–176, Feb. 2014.

[10] Y. Baba and V. A. Rakov, "Electromagnetic models of the lightning return stroke," *J. Geophys. Res.*, vol. 112, no. D4, pp. 1–17, Feb. 2007.

[11] K. Arzag, Z. Azzouz, and B. Ghemri, "Lightning electromagnetic pulse simulation using 3D-FDTD method (comparison between PEC and UPLMBoundary conditions)," in *Proc. 33rd Int. Conf. Lightning Protection (ICLP)*, Sep. 2016, pp. 1–6.

[12] K. Arzag, Z. Azzouz, and B. Ghemri, "Modeling and simulation of the lightning return stroke current using electromagnetic models and the 3D-FDTD method," in *Proc. 6th Int. Conf. Recent Adv. Electr. Syst. (ICRAES)*, vol. 16, 2016, pp. 20–22.

[13] R. Moini, B. Kordi, G. Z. Rafi, and V. A. Rakov, "A new lightning return stroke model based on antenna theory," *J. Geophys. Res., Atmos.*, vol. 105, no. D24, pp. 29693–29702, Dec. 2000.

[14] S. Miyazaki, "Reproduction of electromagnetic fields associated with lightning return stroke to a high structure using FDTD method," in *Proc. IEEJ Nat. Conv.*, no. 7-065, 2004, p. 98.

[15] K. Kutsuna, S. Koike, N. Nagaoka, Y. Baba, and V. A. Rakov, "Wave propagation speed and equivalent impedance of dielectric-coated conductor representing lightning return-stroke channel," *IEEE Trans. Electromagn. Compat.*, vol. 65, no. 2, pp. 601–604, Apr. 2023.

[16] V. Rakov and A. Dulzon, "A modified transmission line model for lightning return stroke field calculations," in *Proc. 9th Int. Symp. Electromagn. Compat.*, 1991, pp. 229–235.

[17] Q. Zhang, D. Li, Y. Zhang, J. Gao, and Z. Wang, "On the accuracy of wait's formula along a mixed propagation path within 1 km from the lightning channel," *IEEE Trans. Electromagn. Compat.*, vol. 54, no. 5, pp. 1042–1047, Oct. 2012.

[18] A. Tatematsu and T. Noda, "Three-dimensional FDTD calculation of lightning-induced voltages on a multiphase distribution line with the lightning arresters and an overhead shielding wire," *IEEE Trans. Electromagn. Compat.*, vol. 56, no. 1, pp. 159–167, Feb. 2014.

[19] Q. Zhang, X. Tang, W. Hou, and L. Zhang, "3-D FDTD simulation of the lightning-induced waves on overhead lines considering the vertically stratified ground," *IEEE Trans. Electromagn. Compat.*, vol. 57, no. 5, pp. 1112–1122, Oct. 2015.

[20] V. Javor, K. M. Lundengård, M. P. Rancic, and S. Silvestrov, "Analytical representation of measured lightning currents and its application to electromagnetic field estimation," *IEEE Trans. Electromagn. Compat.*, vol. 60, no. 5, pp. 1415–1426, Oct. 2018, doi: 10.1109/TEMC.2017.2768549.

[21] Y. Zhang, W. Lü, S. Chen, D. Zheng, Y. Zhang, X. Yan, L. Chen, W. Dong, J. Dan, and H. Pan, "A review of advances in lightning observations during the past decade in Guangdong, China," *J. Meteorological Res.*, vol. 30, no. 5, pp. 800–819, Oct. 2016.
[22] G. Zhang, M. Zhang, and Y.-P. Du, "Representation of lightning return stroke channel in FDTD code and its impact on lightning-produced electric field calculation," in *Proc. 34th Int. Conf. Lightning Protection (ICLP)*, Rzeszow, Poland, Sep. 2018, pp. 1–5, doi: 10.1109/ICLP.2018.8503324.
[23] V. A. Rakov and M. A. Uman, *Lightning: Physics and Effects*. Cambridge, U.K.: Cambridge Univ. Press, 2003.
[24] V. A. Rakov, "Some inferences on the propagation mechanisms of dart leaders and return strokes," *J. Geophys. Res., Atmos.*, vol. 103, no. D2, pp. 1879–1887, Jan. 1998.
[25] D. Shi, D. Zheng, Y. Zhang, Y. Zhang, Z. Huang, W. Lu, S. Chen, and X. Yan, "Low-frequency e-field detection array (LFEDA)—Construction and preliminary results," *Sci. China Earth Sci.*, vol. 60, no. 10, pp. 1896–1908, Sep. 2017.
[26] V. A. Rakov, "Lightning return stroke speed," *J. Lightning Res.*, vol. 1, pp. 80–89, Jan. 2007.
[27] D. Wang, N. Takagi, T. Watanabe, V. A. Rakov, and M. A. Uman, "Observed leader and return-stroke propagation characteristics in the bottom 400 m of a rocket-triggered lightning channel," *J. Geophys. Res., Atmos.*, vol. 104, no. D12, pp. 14369–14376, Jun. 1999.
[28] S. Cai, M. Chen, Y. Du, and Z. Qin, "A leader-return-stroke consistent macroscopic model for calculations of return stroke current and its optical and electromagnetic emissions," *J. Geophys. Res., Atmos.*, vol. 122, no. 16, pp. 8686–8704, Aug. 2017.

GE ZHANG received the B.Eng. degree in electronic information engineering from the Chengdu University of Information Technology, Chengdu, China, in 2015. He is currently pursuing the Ph.D. degree with the Department of Building Environment and Energy Engineering, The Hong Kong Polytechnic University, Hong Kong, China. His research interests include computational lightning electromagnetics and lightning detection.

MINGLI CHEN received the B.Sc. degree in physics from Lanzhou University, China, in 1985, the M.Sc. degree in atmospheric physics from the Chinese Academy of Sciences, in 1988, and the Ph.D. degree in electrical and electronic information from the Gifu University of Japan, in 2000. He was a Researcher with the Lanzhou Institute of Plateau Atmospheric Physics, Chinese Academy of Sciences, from 1988 to 1996. He is currently a Professor with the Department of Building Environment and Energy Engineering, The Hong Kong Polytechnic University. His research interests include lightning physics, lightning detection, and structural lightning protection.

SHAOYANG WANG (Graduate Student Member, IEEE) received the B.Sc. degree in atmospheric science from the University of Science and Technology of China, in 2015, and the M.Sc. degree from the Department of Building Environment and Energy Engineering, The Hong Kong Polytechnic University, in 2020, where he is currently pursuing the Ph.D. degree with the Department of Building Environment and Energy Engineering. His research interests include weak signal detection, data acquisition systems, and lightning observation.

YAN GAO received the B.Sc. degree in atmospheric physics from the University of Science and Technology of China, in 2011, the M.Sc. degree in atmospheric physics from the Chinese Academy of Meteorological Sciences, in 2014, and the Ph.D. degree in electronic engineering from The Hong Kong Polytechnic University, in 2020. His current research interests include the spatial and electromagnetic characteristics of lightning struck to high-rise buildings and tall tower in urban area.

YA-PING DU received the B.Sc. and M.Sc. degrees in electrical engineering from Shanghai Jiao Tong University, China, in 1984 and 1987, respectively, and the Ph.D. degree in electrical engineering from the University of Southern California, USA, in 1994. He is currently a Professor with the Department of Building Environment and Energy Engineering, The Hong Kong Polytechnic University. His research interests include electromagnetic environments, lightning protection, and power quality in electric power systems, electrified railway systems, and buildings.